CFD ANALYSIS OF A HYDROGEN EXPLOSION TEST WITH HIGH IGNITION ENERGY IN OPEN SPACE

Hyung Seok Kang, Sang Baik Kim, Min-Hwan Kim and Hee Cheon NO*

KAERI, Daedeok-daero 1045, Yuseong, Daejeon 305-353,Republic of Korea
**KAIST, Department of Nuclear and Quantum Engineering, 335 Gwahagno, Yuseong, Daejeon 305-353, Korea*

Abstract
A CFD (computational fluid dynamics) calculation for the SRI's hydrogen explosion test was performed to establish an analysis methodology for a hydrogen explosion phenomenon. A spark ignition model to simulate an electric spark of 40J in the SRI's hydrogen explosion test was developed based on an energy conservation law. The CFD analysis can reasonably predict the peak overpressure and flame front TOA (time of arrival) if proper values for the pressure and the radius for the spark ignition model are chosen. A sensitivity calculation for the spark ignition model and grid distribution should be performed to establish the CFD analysis methodology for the hydrogen explosion. However, it is know that the CFD analysis may be used as an accurate evaluation tool to provide the 3-dimesnional information of an overpressure and a time history of the overpressure variation.

1. INTRODUCTION

A Very High Temperature Reactor (VHTR) connected to a hydrogen production facility is being developed at KAERI (Chang, 2007). The VHTR and the hydrogen production facility will be designed and constructed according to Korean regulations and technical standards. One of the regulations may be the safety distance between the VHTR and the hydrogen production facility. This distance is generally determined by the peak overpressure that does not damage a structure or the people near by it (Kang, 2009). A Computational Fluid Dynamics (CFD) code may be a useful tool to predict an overpressure due to a gas explosion because the CFD can simulate a gas leakage from a storage tank, a dispersion into an air environment and the explosion phenomenon continuously (Inba, 2004a; Inba, 2004b; Kang, 2009). The CFD can also analyze the asymmetric explosion phenomenon due to a complicated geometry and a wind effect (Inba, 2004a; Inba, 2004b). Another advantage of the CFD analysis is that it can provide valuable information on an impulse which is defined as the overpressure times the duration of a pressure wave (Bjerketvedt, 1997; Kanninen, 1985; Popat, 1996; Wingerden, 1999). The quantity of the impulse may be used in consideration of the dynamic load (Kanninen, 1985; Wingerden, 1999). A the peak overpressure at a certain location in the CFD analysis can be determined from a time history of the overpressure data.

The CFD analysis was performed to start the development work for the analysis methodology for a hydrogen explosion phenomenon and to predict the peak overpressure distribution inside the tent in the 5.6m^3 mixture volume of hydrogen and air case of the SRI hydrogen explosion tests (SRI, 2002). As a first step, the pressure buildup process by the combustion flame acceleration due to the obstacle inside the tent should be accurately simulated. Otherwise, the pressure wave propagation from the tent region into the far field may not be predicted well. The final goal of the CFD analysis is to develop a complete evaluation tool for a gas leakage from a hydrogen production facility, a hydrogen dispersion, a hydrogen explosion and a blast wave propagation. A commercial CFD code CFX-11 (Ansys, 2008) was used.

2. SRI HYDROGEN EXPLOSION TEST

The SRI performed the hydrogen explosion test in an open space by varying the mixture volume of hydrogen-air, the hydrogen gas concentration, the ignition method and the existence of an obstacle, and they measured the peak overpressure and the flame front Time-Of-Arrival (TOA) inside the tent where the hydrogen gas was located and around the tent (Fig. 1) (SRI, 2002). Also, the peak overpressure at 11m, 21m and 41m from the tent was measured. After the start of the ignition in the experiment, the tent was quickly removed. For a comparison of the measured peak overpressure with the predicted value the CFD results, the selected test cases are a 5.6m^3 volume mixture of hydrogen (about 30 vol. %) and air with an obstacle under a spark ignition of 40J. The stoichiometry reaction of hydrogen and air is expressed as Eq. (1).

$$H_2 + 1/2O_2 \rightarrow H_2O \tag{1}$$

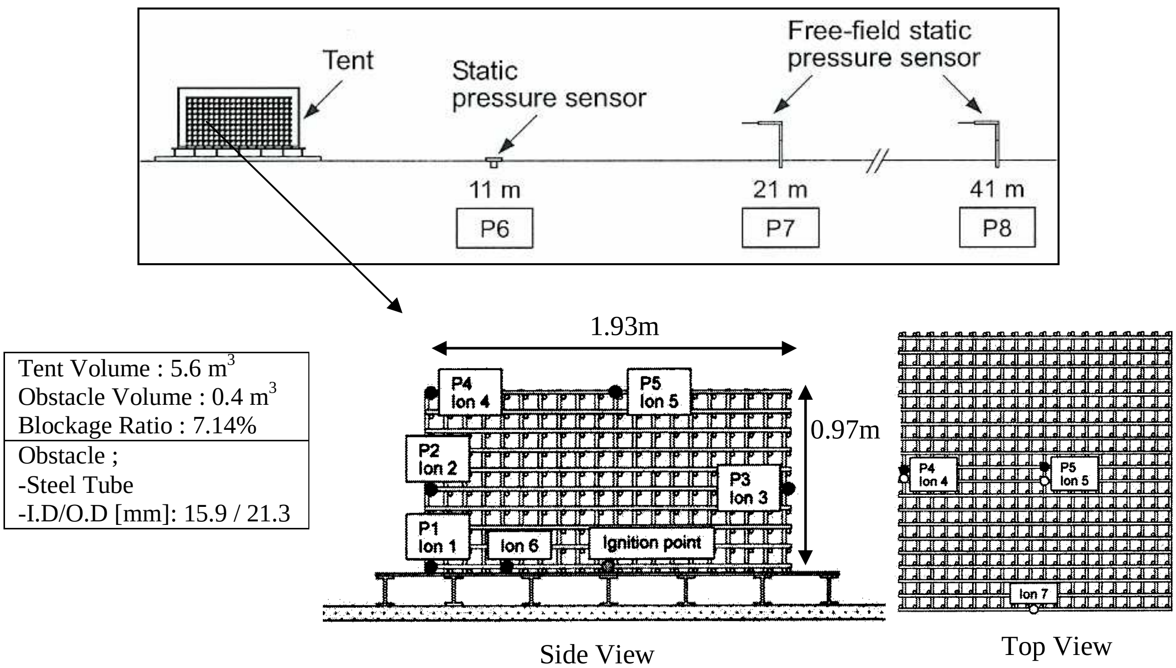

Fig. 1: SRI Hydrogen Explosion Test Facility (SRI, 2002)

3. SRI HYDROGEN EXPLOSION TEST

3.1 Grid Model and Boundary Conditions

A 3-dimensional and half symmetric grid model (Fig. 2) for simulating the tent and its environment was generated based on SRI's test facility (SRI, 2002). A total of 27,808,481 hexahedral mesh cells in the grid model were produced, and a dense mesh cell distribution with a 1cm cell length was located around the tent region (2.51m x 5m x 2.51m) to resolve the rapid propagation of the flame due to the obstacle structure. A coarse mesh cell distribution with a 4cm cell length from the tent region boundary to the far distance of 10m was generated only to assure the pressure wave propagation. This course mesh may not exactly catch the pressure wave propagation. The mesh for the obstacle tube inside the tent was not generated, and the contacted surface of computational domain in the tent to the obstacle tube was treated as a wall boundary condition. A shape of the cylindrical pipe was treated as a rectangular pipe to simplify the grid generation work to maintain the volume of the obstacle in the grid model the same as that of the test. An opening condition (Ansys, 2008) was applied to all the surrounding surfaces except for the bottom surface, which can simulate the pressure wave passing and allows for an inflow and outflow of a fluid through the surfaces.

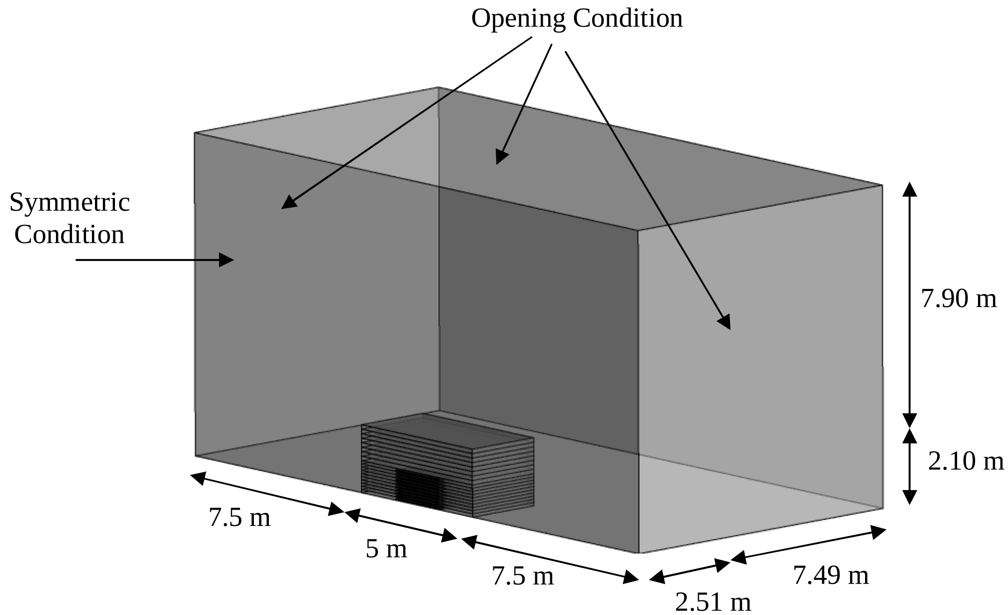

(a) Computational domain (1/2 symmetric model)

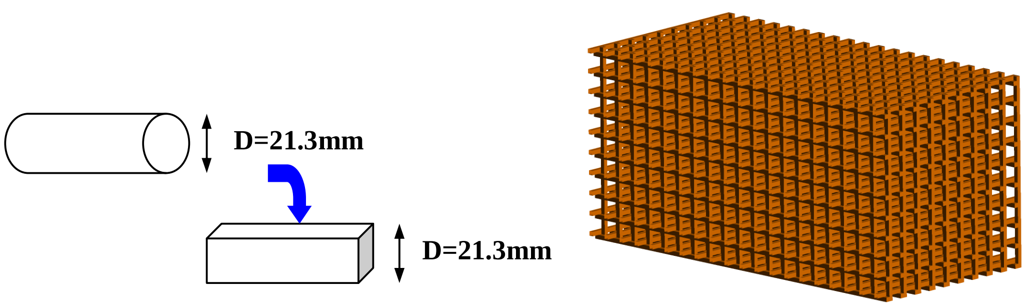

(b) Obstacle model

Fig. 2: Grid Model and Boundary Conditions for the CFD analysis

3.2 Development of a Spark Ignition Model and Initial Condition

An electric spark device was used to ignite a mixture of hydrogen and air in the SRI explosion test. The equivalent energy for the spark operation was reported as 40 J (SRI, 2002). This value is very large when compared to the spark ignition energy of about 10 mJ in an ordinary combustion test (Heywood, 1988). The excessive energy may enlarge an activated region in which the temperature and pressure of the mixture of hydrogen and air is greatly increased from the initial values of 1bar and 283.75K (SRI, 2002). Then the combustion may simultaneously take place over the whole activated region. The combustion at the enlarged region may reduce the transition time from the laminar flame to the turbulent flame because an instability phenomenon may be easily developed in case of the large radius of combustion flame (Bradly, 2007).

In order to model this ignition process, the effective spark ignition model representing the pressure, the temperature and the volume of the activated region due to a spark was introduced because the local phenomena of the spark and the ignition process of the flame are too complicated to exactly model (Heywood, 1988; Kang, 2009). Therefore, a spherical activated region model based on the energy conservation under the assumption of an adiabatically confined condition was introduced in Eq. (2) (Kang, 2009).

$$\begin{aligned} E_{spark} = m_{act}\overline{C_p}(T_h - T_c) &= V_{act}\rho_m \overline{C_p}(T_h - T_c) \\ &= V_{act}(\rho_{m,h}C_{p,h}T_h - \rho_{m,c}C_{p,c}T_c) \\ &= V_{act}(\frac{P_h}{R_g}C_{p,h} - \frac{P_c}{R_g}C_{p,c}) \\ &= \frac{V_{act}}{R_g}(P_hC_{p,h} - P_cC_{p,c}). \end{aligned} \tag{2}$$

The ideal gas law (P=ρRT) is used in the derivation of Eq. (2) to represent the spark energy in terms of two unknown variables of the pressure (P_h) and the spherical volume (V_{act}) of the activated mixture of hydrogen and air. The local temperature range of the activated volume due to the spark may be assumed to be from 2,000K to 6,000K based on the experimental results (Heywood, 1988). However, from the available specific heat capacity data for a mixture of hydrogen and air it is from 2,000K to 3,000K (Turns, 2000). Thus, the specific heat capacity of the mixture of hydrogen and air at 2,000K and 3,000K are substituted separately into Eq. (2) to set up a sensitivity calculation conditions as shown in Fig. 9.

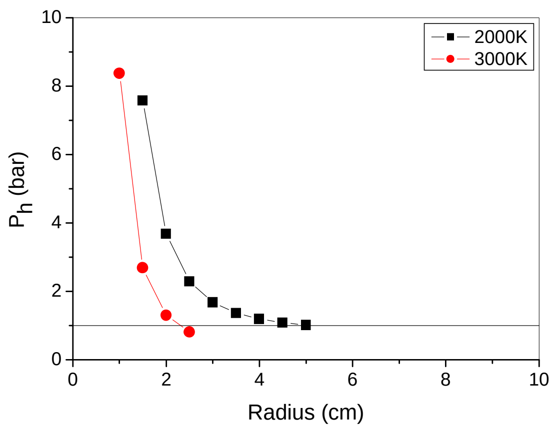

Fig. 3: Calculated Range of Pressure and Radius of Activated Spherical Volume due to spark (40J)

As the first calculation of sensitivity conditions (Fig. 3), the selected radius, temperature and pressure of the activated region are 4cm, 2,000K and 119kPa respectively. These values are given as the initial condition of CFD calculation such Fig. 4. The CFD analysis with this spark ignition model will be validated through comparison work of the test data with the CFD results for the peak overpressure and the flame speed around the tent. Also, the stoichiometry gas distribution of hydrogen, oxygen and nitrogen was given to the tent volume in the grid model as the initial condition.

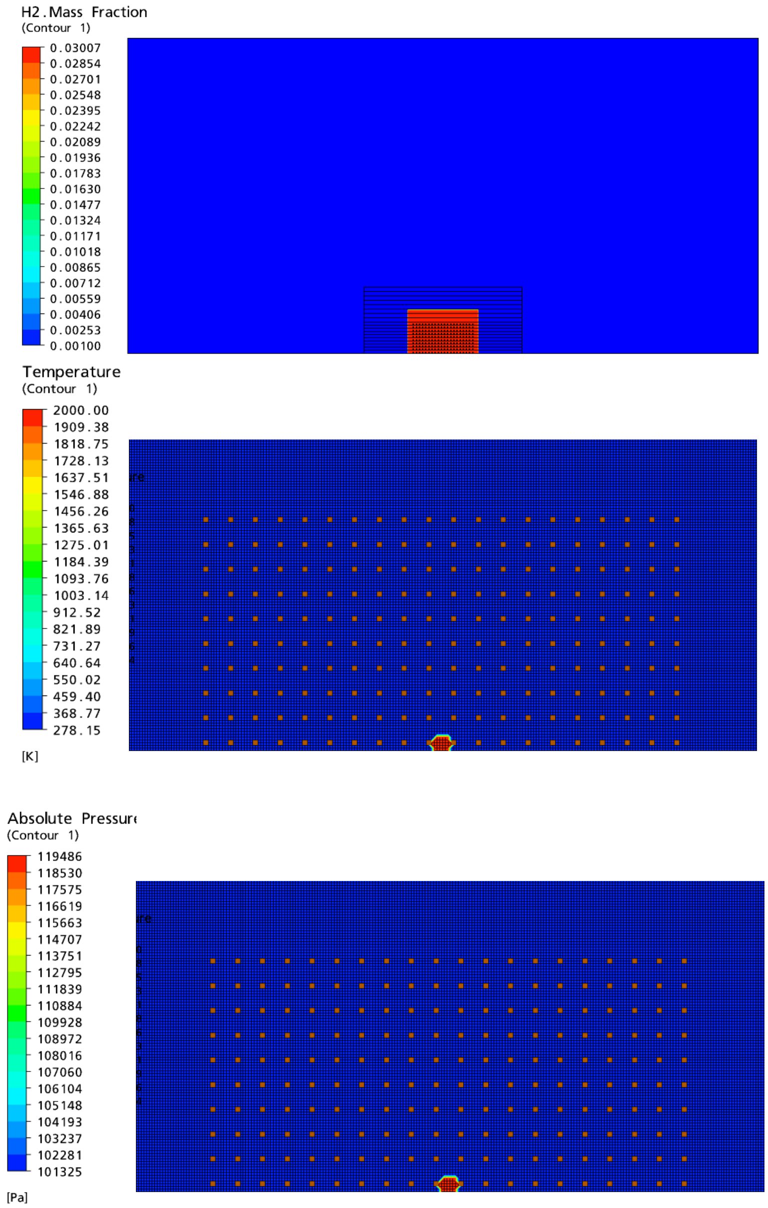

Fig. 4: Initial conditions for the CFD analysis
(H_2 vol.% =30, P_h=119kPa, R=4cm, T=2,000K)

3.3 Flow Field Models and Combustion Model

The hydrogen combustion phenomenon in the obstacle structure was treated as a compressible flow, a combustion flow, a turbulent flow, a buoyant flow and a transient flow. The governing equations (Eq. (3) ~ (7)) used in this study are the Navier-Stokes, the energy and the species transport equations with a coupled solver algorithm (Ansys, 2008). Turbulent flow was modeled by the standard k-ε turbulent model (Eq. (8) ~ (9)), and the buoyancy flow was modeled by the full buoyancy model (Ansys, 2008). And also, the discrete transfer model (Eq. (10)) with the gray spectral model (Ansys, 2008; Coelho, 1997; Modest, 1993) was used for the simulation of the radiative heat transfer. A radioactive gas absorption by the diatomic elements of H_2O was considered with the Plank-mean gas absorption coefficient (Modest, 1993). The transient calculation for a total time of 0.05 seconds with a time step of 0.0001~0.005 seconds was performed to capture the pressure wave phenomenon which may disappear in a very short time.

The Eddy Dissipation Model (EDM) (Ansys, 2008; Hjertager, 1982), modified from the Eddy Break-Up (EBU) model (Spalding, 1976), was used for the one step combustion reaction of the hydrogen and air mixture. The global reaction rate of the EDM was chosen as the slowest reaction rate of a fuel, an oxidant and a product. Each reaction rate was proportional to a turbulent quantity ratio (ε/k), a mass fraction (Y_f, Y_o, Y_p), model constants (A=8, B=0.75) and a stoichiometry coefficient (r_f) (Ansys, 2008). The global reaction rates and the reaction rate of the fuel, the oxidant and the product were defined such as Eq. (11) ~ Eq. (13).

$$\frac{\partial \rho}{\partial t} + \nabla \bullet (\rho \vec{V}) = 0 \tag{3}$$

$$\frac{\partial (\rho \vec{V})}{\partial t} + \nabla \bullet (\rho \vec{V} \otimes \vec{V}) = -\nabla p + \nabla \bullet \left[\mu_{eff} \left(\nabla \vec{V} + (\nabla \vec{V})^T\right)\right] + (\rho - \rho_{ref})\vec{g} \tag{4}$$

$$\mu_{eff} = \mu + C_\mu \rho \frac{k^2}{\varepsilon} \tag{5}$$

$$\frac{\partial (\rho h_{tot})}{\partial t} - \frac{\partial p}{\partial t} + \nabla \bullet (\rho \vec{V} h_{tot}) = \nabla \bullet \left(\lambda \nabla T + \frac{\mu_t}{\Pr_t} \nabla h\right) + \nabla \bullet (\vec{V} \bullet \tau) \tag{6}$$

$$\frac{\partial (\rho Y_i)}{\partial t} + \nabla \cdot (\rho \vec{V} Y_i) = \nabla \cdot \left(\rho D_{i,m} + \frac{\mu_t}{Sc_t}\right) \nabla Y_i + R_i \tag{7}$$

$$\frac{\partial (\rho k)}{\partial t} + \nabla \bullet (\rho \vec{V} k) = \nabla \bullet \left[\left(\mu + \frac{\mu_t}{\sigma_k}\right) \nabla k\right] + P_k - \rho \varepsilon \tag{8}$$

$$\frac{\partial (\rho \varepsilon)}{\partial t} + \nabla \bullet (\rho \vec{V} \varepsilon) = \nabla \bullet \left[\left(\mu + \frac{\mu_t}{\sigma_\varepsilon}\right) \nabla \varepsilon\right] + \frac{\varepsilon}{k}(C_{\varepsilon 1} P_k - C_{\varepsilon 2} \rho \varepsilon) \tag{9}$$

$$\frac{dI_\nu(r,s)}{ds} = -(K_{a\nu} + K_{s\nu}) I_\nu(r,s) + K_a I_b(\nu, T) + \frac{K_{s\nu}}{4\pi} \int dI_\nu(r, s') \Phi(s \bullet s') d\Omega' + S \tag{10}$$

$$R_f = A\rho \frac{\varepsilon}{k} (Y_f) \tag{11}$$

$$R_o = A\rho \frac{\varepsilon}{k} \left(\frac{Y_o}{r_f}\right) \tag{12}$$

$$R_p = AB\rho \frac{\varepsilon}{k} \left(\frac{Y_p}{1 + r_f}\right) \tag{13}$$

3.4 Discussion on the CFD Analysis Results

A CFD calculation with the developed spark ignition model was performed to find a proper analysis methodology for the hydrogen explosion phenomenon through a comparison of the CFD results with the test results for the peak pressure and the flame front TOA around the tent. All the residuals of the Navier-Stokes, the energy, the standard k-ε turbulent and the gas species equations were converged to below 10^{-4}. The CFD results of temperature distribution (Fig. 5) according to the time pass show that the combustion flame slowly propagates over a distance of about 0.4m from the point “A” to “B” for

0.005 ~ 0.03 seconds, but is accelerated along the distance from the point “B” to “C” for 0.03 ~ 0.04 seconds. The reason of this acceleration may be explained by the flame speed being directly proportional to a force developed behind the flame front surface, where the force is produced by the product of the pressure due to the combustion energy and the surface area took up by the flame front. Thus, the flame acceleration may be easily developed as long as there occurs a flame area splitting due to the obstacle structures.

The overpressure results of the CFD calculations (Fig. 6) show that the peak overpressure is gradually increased from the initial value of 119 kPa to 124 kPa at 0.03 seconds as the combustion phenomenon takes place. However, the peak pressure peaks into 472 kPa at 0.04 seconds because most of hydrogen located inside the tent is burnt out at time step of 0.03 ~ 0.04 seconds. The overpressure history at the pressure sensor locations of P1, P2, P4 and P5 of the CFD results are shown in Fig. 7. The passing time of all pressure waves at each location are calculated to be about 0.0037 ~ 0.0041 seconds. The calculated magnitudes of all pressure waves are maintained around 500 kPa, and the pressure build-up phenomenon between the pressure sensors is not found in the CFD calculation.

In the test results, the pressure build-up process for a short distance of 0.1 ~ 0.3m was clearly measured at very small time duration of about 0.0004 seconds (Fig. 7). This difference between the CFD results and test results may be resolved by a mesh sensitivity calculation with a denser grid model because the propagation of an instant pressure wave may depend on the cell length in the grid model. Also, the comparison of the flame front TOA between the CFD results and the test results (Fig. 8~9) indicate that the predicted value by the CFD analysis are about 0.015 seconds slower than those measured in the test. Moreover, the passing time from the ionization sensor 6 to the ionization sensor 7 predicted by the CFD analysis is as much as 7 times longer than that of the test results.

The CFD results and the test data of the average and the maximum peak overpressure and the flame front TOA are shown in Table 1. As a result of the comparison of the CFD results and the test data, we can see that the physical phenomena of the overpressure and flame front TOA in the CFD results with the spark ignition model (r = 4cm, P_h = 119kPa, T_h = 2,000K) simulate well the physical behaviour of the test results, but the CFD results do not accurately predict the measured value in the test results. The difference between the CFD results and the test data for the overpressure and flame front TOA is about 100 ~ 150 %. Thus, as a first thing, the sensitivity CFD calculation by varying the parameters of spark ignition model should be performed to accurately predict the flame front TOA of test results because the pressure distribution is usually determined by an amount of volume and time span for completing the combustion in a certain space. After finding the best parameter of the spark ignition model, the grid sensitivity calculation may be necessary because the decay of pressure wave magnitude is generally dependent on the mesh distribution.

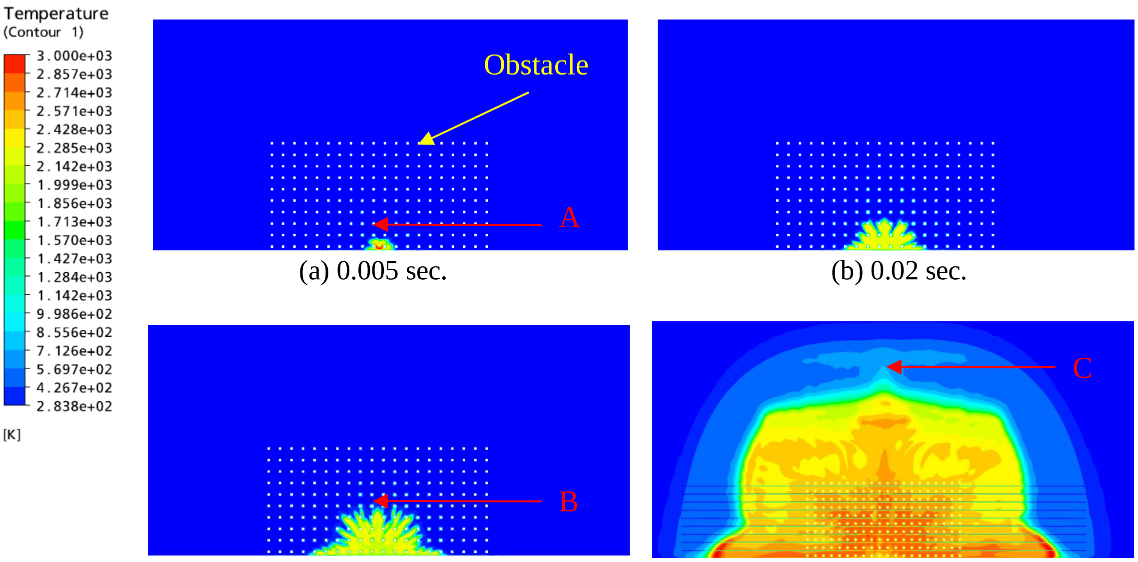

(a) 0.005 sec. (b) 0.02 sec.

(c) 0.04 sec. (d) 0.04 sec.

Fig. 5 : Temperature distributions on the center plane by the CFD analysis

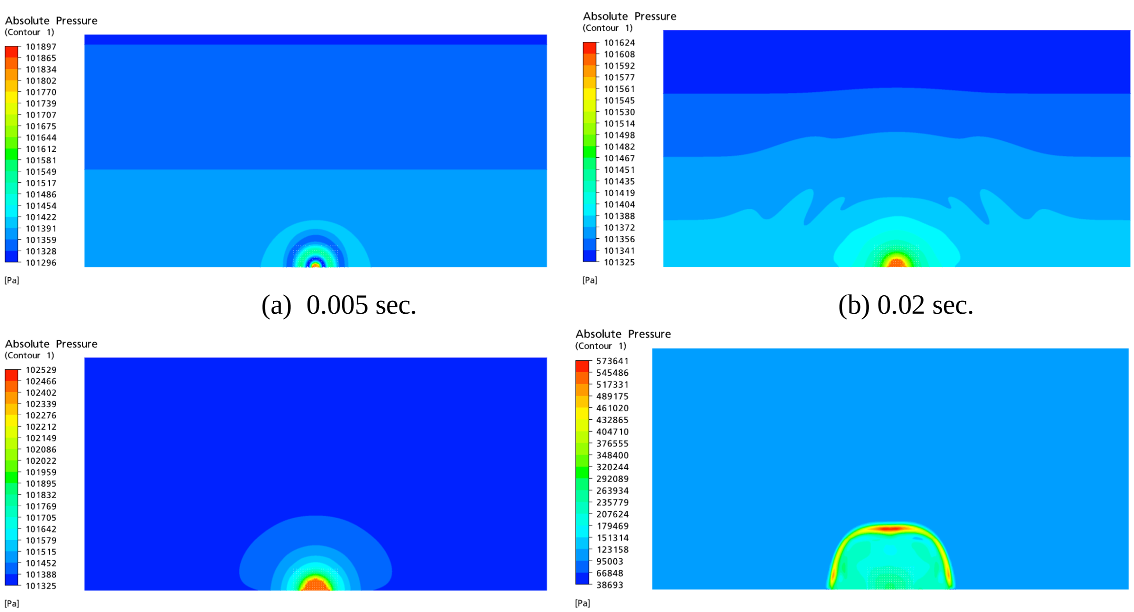

(a) 0.005 sec. (b) 0.02 sec.

(c) 0.03 sec. (d) 0.04 sec.

Fig. 6: Pressure distributions on the center plane by the CFD analysis

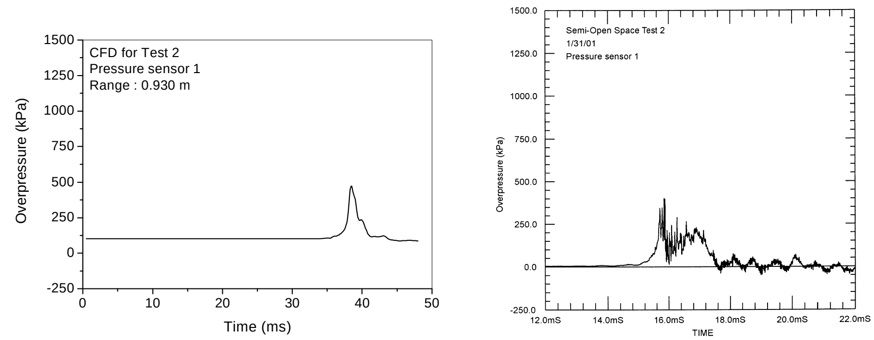

(a) P1 Location

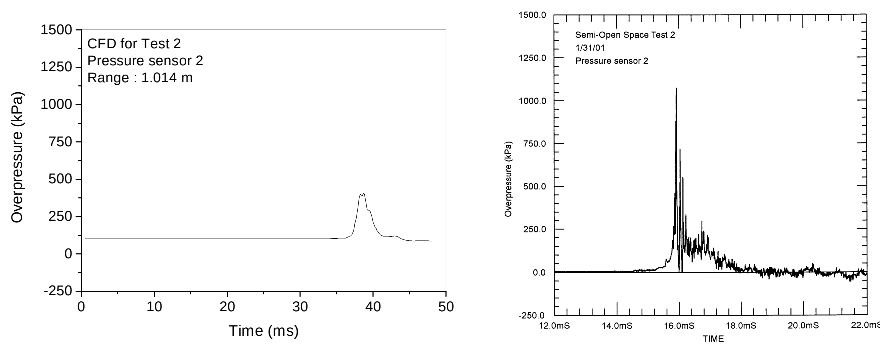

(b) P2 Location

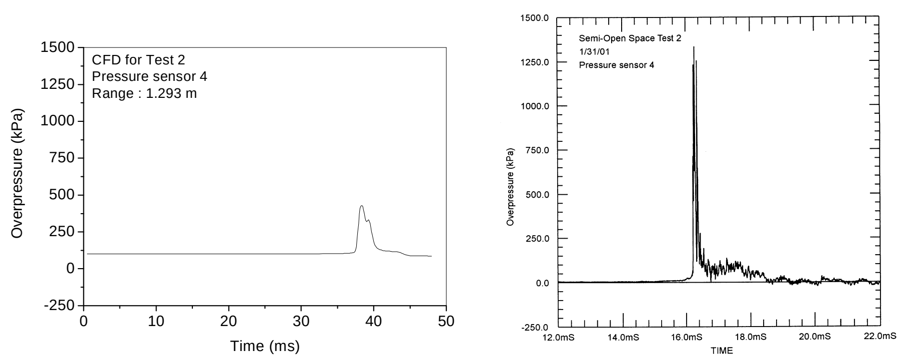

(c) P4 Location

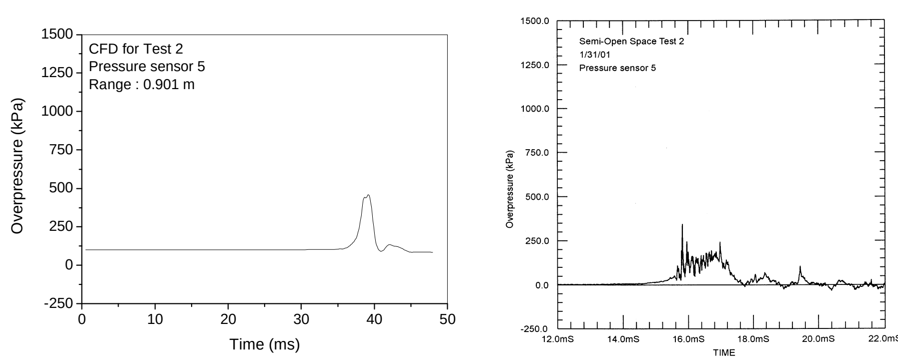

(d) P5 Location

Fig. 7: Comparison of overpressure at the pressure sensor 5 locations between the CFD results and the test results (SRI, 2002)

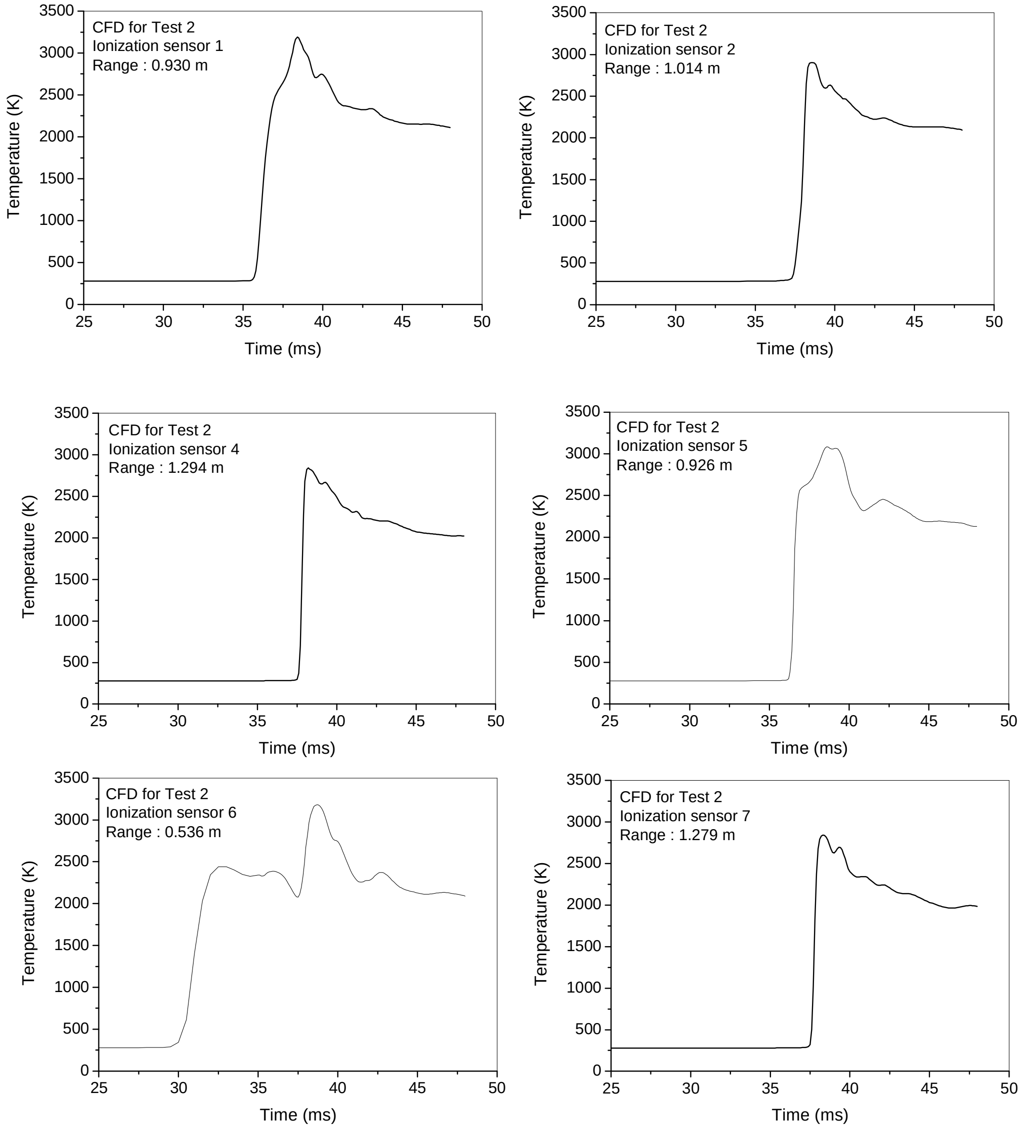

Fig. 8: CFD results of Flame Front Time-Of-Arrival (TOA) at Ionization Sensor Locations

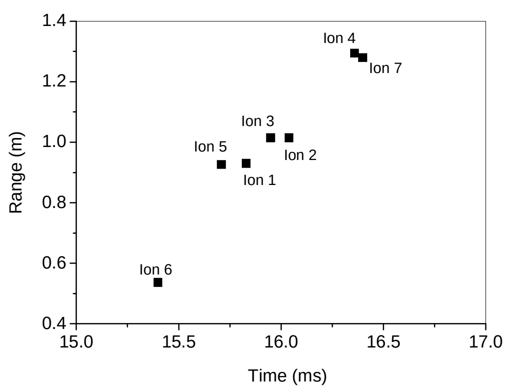

Fig. 9: Test results of Flame Front Time-Of-Arrival (TOA) at Ionization Sensor Locations (SRI, 2002)

Table 1. Comparison of overpressure and flame speed inside tent region between CFD results and Test Results (SRI, 2002)

	Overpressure	Flame Speed*
CFD	-Average : 441.8 kPa -Maximum : 473.1 kPa	-Average : 27.0 m/s -Maximum : 34.1 m/s
Test	-Average : 781.3 kPa -Maximum : 1,072.3 kPa	-Average : 62.3 m/s -Maximum : 79.1 m/s

*Definition of Flame Speed : distance from ignition point to ionization sensor location is divided by flame front TOA

4. CONCLUSIONS AND FURTHER WORK

According to the CFD analysis results for the SRI's hydrogen explosion test, it is concluded that the CFD analysis can reasonably predict the peak overpressure and flame front TOA if proper values for the pressure and the radius for the spark ignition model are chosen. Therefore, the CFD analysis may be used as an accurate evaluation tool to provide the 3-dimesnional information on a peak overpressure and the time history of an overpressure variation. However, the sensitivity calculation for the spark ignition model and grid distribution should be performed to establish the CFD analysis methodology for the hydrogen explosion.

REFERENCES

B. H. Hjertager, Simulation of Transient Compressible Turbulent Reactive Flows, Combustion Science and Technology, 27, 159-170 (1982).

CFX-11.0 Manual, Ansys Inc. (2008).

D. B. Spalding, Mathematical Models of Turbulent Flames; A Review, Combustion Science and Technology, 13, 3-25 (1976).

D. Bjerketvedt, J. R. Bakke, K. van Wingerden, Gas Explosion Handbook, Journal of Hazardous Materials, 52, pp.1-150 (1997).

D. Bradly, M. Lawes, Kexin Liu, S. Verhelst and R. Woolley, Laminar Burning Velocities of Lean Hydrogen-Air Mixtures at Pressure up to 1.0 MPa, Combustion and Flame 149, 162-172 (2007).

John B. Heywood, Internal Combustion Engine Fundamentals, 427-443, McGraw-Hill (1988).

J. H. Chang, Y. W. Kim, K. Y. Lee. Y. W. Lee, W. J. Lee, J. M. Noh, M. H. Kim, H. S. Lim, Y. J. Shin, K. K. Bae and K. D. Jung, "A Study of a Nuclear Hydrogen Production Demonstration Plant," Nuclear Engineering and Technology, **39,** No.2, pp.111-122 (2007).

M. F. Kanninen and C. H. Popelar, Advanced Fracture Mechanics, Chapter 4, Oxford Engineering Science Series 15, Oxford University Press (1985).

Michael F. Modest, Radiative Heat Trnasfer, 2nd, McGraw-Hill (1993).

N. R. Popat, C. A. Caltin, B. J. Lindstedt, B. H. Hjertager, T. Solberg, O. Saeter and A. C. van den Berg, Investigation to Improve and Asses the Accuracy of Computational Fluid Dynamic Based Explosion Model, Journal of Hazardous Materials, 45, 1-25 (1996).

H. S. Kang, S. B. Kim, M.-H. Kim, W.-J. Lee, and H. C. NO, Regulatory Issues on the Safety Distance between a VHTR and a H_2 Production Facility and an Overpressure Prediction Using Correlations and a CFD Analysis for the JAEA Explosion Test in an Open Space, Nuclear Technology, Vol. 166 No. 1, 86-100 (2009).

K. van Wingerden, O. R. Hansen and P. Foisselon, Predicting Blast Overpressures Caused by Vapor Cloud Explosions in the Vicinity of Control Rooms, Process Safety Progress, 18**,** No.1**,**.17-24 (1999).

P. J. Coelho and M. G. Carvalho, A Conservative Formulation of the Discreter Transfer Model, Journal of Heat Transfer, 119, 118-128 (1997).

SRI, Annual Report on Hydrogen Safety in the World Energy Network (WE-NET), Annual Report (2002).

S, R. Turns, An Introduction to Combustion, 2nd, McGraw-Hill (2000)

Y. Inaba, T. Nishihara and Y. Nitta, Analytical Study on Fire and Explosion Accidents Assumed in HTGR Hydrogen Production System, Nuclear Technology, 146, pp.49-57 (2004a).

Y. Inaba, T. Nishihara, M. A. Groethe and Y. Nitta, Study on explosion characteristics of natural gas and methane in semi-open space for the HTTR hydrogen production system, Nuclear Engineering and Design, 232, 111-119 (2004).